Turkish Journal of Electrical Engineering & Computer Sciences

http://journals.tubitak.gov.tr/elektrik/

Research Article

Turk J Elec Eng & Comp Sci
(2016) 24: 5043 – 5054

doi:10.3906/elk-1412-148

Studies on the application of wavelet families for a high impedance fault location algorithm in a distribution network

Mohd Syukri ALI[1,*], Ab Halim ABU BAKAR[1], Chia Kwang TAN[1], Hazlie MOKHLIS[1,2], Hamzah AROF[2]

[1]UM Power Energy Dedicated Advanced Centre, Level 4, Wisma R&D UM, Jalan Pantai Baharu, University of Malaya, Kuala Lumpur, Malaysia

[2]Department of Electrical Engineering, Faculty of Engineering, University of Malaya, Kuala Lumpur, Malaysia

Received: 23.12.2014 • **Accepted/Published Online:** 25.10.2015 • **Final Version:** 06.12.2016

Abstract: Detecting high impedance faults in a distribution network is a great challenge and locating one is even more challenging. This paper will present an enhanced high impedance fault location algorithm based on the database technique. This paper is an extension of a faulty section identification algorithm developed previously. However, in this paper, the performance of the previous algorithm is investigated first in terms of different sampling rate and window size. Then these parameters will be used as a standard parameter to study the effectiveness of different types of mother wavelets. Each mother wavelet will be used to extract important features of a voltage signal from a single measurement point in a typical 38-node underground distribution network.

Key words: High impedance fault, fault location, mother wavelet, sensitivity analysis

1. Introduction

A high impedance fault (HIF) is defined as a fault in which the fault current is small but may intrude into the region of the full load current. Very frequently, the fault current from a HIF is not sufficient to be detected by the conventional overcurrent protection relays or fuses. The term "high impedance" indicates that there is a large resistance that deters the current flow through the line or cable [1]. The common scenarios that can cause HIF are insulation failure, such as cable degradation due to moisture, contamination on an insulator, and defects on the outer protective cable shield.

Since a HIF is an undesirable event that jeopardizes the power system operation, it is of utmost importance for these HIFs to be speedily located to facilitate supply restoration. However, given that it is already difficult to detect a HIF by the relays, the determination of its fault location is even more challenging. The most challenging problems encountered in locating the fault for a power distribution system is the presence of a lateral with branches, which frequently lead to multiple possible points of fault [2,3]. Any incorrectly identified fault location will delay the supply restoration process.

Numerous studies have been conducted to locate the common faults in the distribution system. Intelligent techniques are among the most popular approaches. In [4–7], an artificial neural network (ANN) was used for fault localization in the distribution network. In [4,5], the fundamental frequency components of voltage and

*Correspondence: mosba86@yahoo.com.my

current were employed. A combination of ANN and support vector machine (SVM) was proposed in [5], whereas in [6,7], the high frequency components were extracted from the faulted waveform to facilitate fault location. Wavelet analysis was performed to extract the features that were the input for training the ANN. In [6], the approximate coefficient of peak-to-peak voltage-to-current ratio was used as the input. In contrast, the zero sequence and maximum value of the discrete wavelet transform decomposition for phases A, B, and C of the postdisturbance voltage and current signals were utilized in [7].

Besides the ANN approaches, the travelling wave technique can provide very accurate results in locating the fault distance for the transmission line [8]. However, it is difficult to implement in a distribution system due to the complexity of a distribution network comprising laterals with many branches [9]. Despite the difficulties, numerous studies have been conducted in recent years to identify the fault location in distribution systems using the travelling wave technique [10,11]. In order to utilize this method, a high sampling rate is required. The most common travelling wave technique is time-domain reflectometry (TDR), in which the reflected waveforms from the faulted point are analyzed [12]. Unfortunately, due to the multiple reflections from the faulted point and also the tee-connections in the distribution network, the measured waveforms are difficult to interpret. Therefore, intense research is ongoing to interpret and simplify the complex waveforms for fault location in the distribution network.

In [13–15], the energy content around the characteristic frequencies of the travelling waves are observed for the transient waveforms. Continuous wavelet transform was incorporated in [13,14] to extract the peak values of the energy spectrum around the path characteristic frequencies (PCFs) to determine the fault location. On the other hand, the authors in [15] proposed that the level of discrete wavelet transform (DWT) with the most energy concentration be selected first and then applied to TDR to identify the fault location in a radial distribution system. In [12], the energy content obtained from multiresolution analysis (MRA) around the PCF was used as input for training the ANN to estimate the fault location. However, the main disadvantage is the requirement of a huge amount of input data to be trained to represent one fault location. A combination of wavelet analysis and support vector regression (SVR) was presented in [16]. The wavelet transform modulus maxima and arriving time of zero and aerial mode components of travelling wave were extracted by wavelet transform to be used as input data for training the SVR to predict the location of the fault. In contrast, the authors in [17] proposed to use a combination of wavelet analysis as the feature extractor together with an ANN and fuzzy logic system to detect the fault types and locations.

It must be noted that most of the available fault location techniques are designated for locating low impedance faults. In comparison, research dedicated to locating HIFs is relatively less common. Due to this reason, prior research was conducted to estimate the faulty section for HIF and was presented in [18]. This paper is an extension of the algorithm presented by the authors in [18], where enhancements are proposed to further improve the previous fault location algorithm. Parameters such as sampling rates and mother wavelets in the previous algorithm are first varied. The parameters that delivered the least number of undefined cases are then shortlisted. Sensitivity studies are then conducted for the algorithm with the shortlisted parameters to evaluate the performance in practical scenarios. The sensitivity study analyzes the variation of the faulted points along the line section as well as changes in the fault impedance values.

In this paper, the fault location for a single line-to-ground fault with high fault impedance is investigated in a radial distribution network consisting of 35 line sections. The proposed algorithm requires only a single measurement for the 3-phase voltages in the distribution network. The database fault location approach is adopted to identify the faulty section. The voltage is first decomposed using the DWT-based MRA technique

for feature extractions. The extracted features are then compared with the values in the database using the average of absolute difference (AAD) approach. Subsequently, the estimated faulty section is determined based on the lowest score of AAD value. The simulation is carried out using PSCAD/EMTDC software and the analysis is performed using MATLAB.

2. Introduction to wavelet transform

Wavelets are mathematical functions that decompose the signal into several frequency components. Then each component is analyzed with a resolution that matches its scale. In other words, wavelets can be expressed as a short wavelike function that can be scaled and translated [19]. In wavelet transforms, the original signals, such as images and waveforms, are represented in terms of scaled and translated wavelets. It allows the features of the signal to be manipulated in different scales independently, such as strengthening or suppressing some particular features. The main advantage of wavelet transform is its capability in analyzing signals containing discontinuities or sharp spikes.

There are several types of wavelet families. Each of the wavelet families can be differentiated based on several main criteria such as [19]:

- The support of wavelet function, ψ, and scaling function, ϕ. The time and frequency localization is quantified based on the convergence speed to 0 of ψ when the time, t, and frequency, ω, progress to infinity.
- The symmetry, which is important to avoid dephasing in image processing.
- The number of vanishing moments for ψ and ϕ, which is significant for compression purposes.
- The regularity in which it is important to get nice features such as smoothness of the reconstructed image or waveform, and also for an estimated function in nonlinear regression analysis.

Each wavelet family contains wavelet subclasses that can be distinguished by the number of vanishing moments. The number of vanishing moments is directly related to the number of coefficients. For example, a Daubechies wavelet family with 4 vanishing moments means that it consists of 4 coefficients and it is called Db4.

In wavelet transform, the original signal will be decomposed by 2 complementary filters, which are called the decomposition low-pass filter and high-pass filter. The scaling function, ϕ, is used for decomposing the low-pass filter and the wavelet function, ψ, is used for decomposing the high-pass filter. The result of the filtering will generate 2 signals called the low-frequency component and the high-frequency component. The low-frequency component is also known as the *approximation signal* and is produced when the original signal is decomposed using the low-pass filter, whereas the high-frequency component is commonly called the *detail signal* and is produced when the original signal passes through the high-pass filter.

3. System modeling

The schematic diagram of the distribution network used in the prior work in [18] as well as in this study is shown in Figure 1. Electrical power is supplied from the 132/11 kV transformer and is distributed radially to 38 nodes. From the network, a total of 35 line sections can be formed. The frequency of the system is 50 Hz.

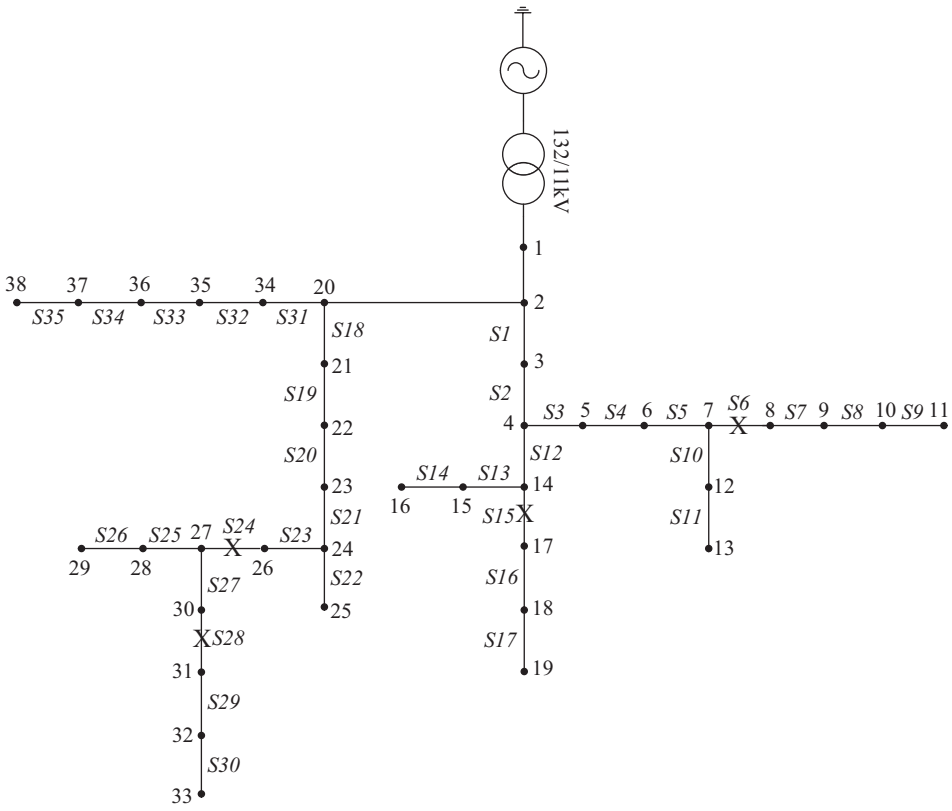

Figure 1. Schematic diagram of a 132/11 kV distribution network.

Power system faults in the distribution network were simulated using PSCAD software. The 3-phase sinusoidal voltage signal is measured at the single measurement point located at the first node. The measured voltage signal is then analyzed using the DWT-based MRA. The algorithm for DWT-based MRA was programmed in MATLAB. Only a single line-to-ground fault (SLGF) is considered in this analysis due to the high probability of this fault occurrence (more than 70% of faults are SLGF [20]) in the system.

4. Proposed method for HIF faulty section

In [18], the AAD approach for HIF faulty section identification was adopted utilizing the detail coefficients feature extracted from wavelet transform. In this approach, the database technique is used, in which the extracted features are compared with the values in the database. The line section that gives the lowest score of AAD value is considered as the faulty section.

A simplified diagram for the distribution system is shown in Figure 2. Initially, the databases are developed by simulating predefined HIF values (40, 50, 60, 70, 80, 90, and 100 Ω) at each node in the distribution system as shown in Figure 1. In each simulation, the voltage waveform is measured at node 1 and it is subsequently analyzed using wavelet transform. The average of the extracted detail coefficients of voltage signal between 2 neighboring nodes is calculated and stored as a database for that particular line section. The average value can be calculated as follows:

$$Average = \frac{\sum d_i + \sum d_j}{2},$$

where:

$\sum d_i$ = Summation of detail coefficients of node i.

$\sum d_j$ = Summation of detail coefficients of node j. Node i and j are adjacent nodes.

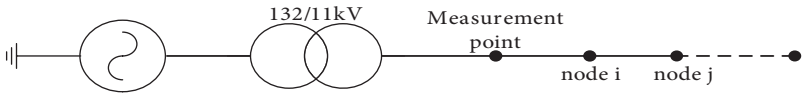

Figure 2. Simple diagram of distribution network.

When the fault is tested in the distribution system, the faulty section can be estimated by comparing the extracted features of the measured signal with the databases. It can be compared based on the AAD calculation. The AAD scores can be calculated as follows:

$$AAD_m = \frac{\sum_{i=1}^{n} \left| \sum d_{i(measured)} - r_{mi} \right|}{n},$$

where:

m = 1,2,. . . .,35 (number of line section).

n = number of data to be compared.

$\sum d_{i(measured)}$ = sum of detail coefficients of the test voltage signal.

r_{mi} = reference database/average data stored in the database.

Once the AADs for all entries in the database have been calculated, they are arranged from the smallest to highest value where the smallest value is ranked as the first. The first rank indicates the highest probability of HIF occurrence at that line section. Therefore, the line section that gives the lowest AAD score is first considered as the faulty section.

4.1. An enhanced algorithm through comparative studies

In this analysis, selected parameters in the algorithm proposed previously in [18] are varied. Subsequently, the impacts of the varied parameters on the accuracy of the algorithm in identifying the faulty section are compared and analyzed. The results presented in the previous work in [18] serve as the benchmark for comparison purposes in this study. The 2 parameters being varied in this algorithm are:

1. Sampling rate and window size for the feature extraction using wavelet transform.
2. Type of wavelet family and mother wavelet in the wavelet transform.

The mother wavelet with the highest accuracy is then identified based on the findings from this comparative study.

4.1.1. Change in sampling rate and window size

In this section, the sampling rate for DWT decomposition as well as the window size for feature extraction are varied. The authors in [21] proposed a higher sampling rate to analyze the signal. However, a higher sampling rate will slow down the simulation speed due to excessive data transfer from EMTDC to PSCAD. In contrast, a lower sampling rate will cause the waveform to look 'shabby'.

The algorithm proposed previously considered a sampling rate of 6.4 kHz. In contrast, this algorithm proposes a lower sampling rate of 4 kHz. Besides that, 256 samples or 2 cycles of the voltage waveform are used for the feature extraction in the previous algorithm. However, the present algorithm proposes 128 samples, which is equivalent to 1.6 cycles of the voltage waveform. In this analysis, a lower sampling rate and a lower number of samples are considered in order to reduce the size of memory needed to store the voltage data and to expedite the analysis time, respectively.

A comparison of the varied sampling rate and window size between the previous and present algorithms is shown in Table 1. The same simulations as conducted previously in [18] are repeated using this new algorithm. The Db4 mother wavelet proposed previously remained unchanged in this study. A total of 6 different HIFs with fault impedance values of 45 Ω, 55 Ω, 65 Ω, 75 Ω, 85 Ω, and 95 Ω are applied in the middle of each line section. Both previous and present algorithms are then executed for each of the fault simulations with varying fault impedance and fault location. For each execution, both algorithms rank the possible faulted sections in a sequence of rank 1, rank 2, rank 3, and undefined.

Table 1. Simulation data.

	Previous simulation	Current simulation
Channel plot step	156 μs (128 samples per cycle)	250 μs (80 samples per cycle)
Sampling frequency	6.4 kHz	4 kHz
Number of samples for analysis	256 samples (consists of the 1st and 2nd full cycles of postdisturbance voltage signal)	128 (from the point of fault occurrence)

The first rank represents the most probable faulted section. If the fault is not identified in the first rank section, then the second followed by the third estimated faulty section is checked for the fault. The undefined faulty section is marked 'X' and is classified when the fault is not found in the sections ranked 1, 2, or 3. After completing 35 fault simulations for each of the fault impedances, the number of correctly ranked faulted sections are computed for each of the ranks. The numbers of correctly ranked faulted section results for both algorithms are tabulated in Table 2 for comparison purposes.

Table 2. Number of correctly identified faulty sections in each rank.

Ranking	Previous results						Current results					
	45 Ω	55 Ω	65 Ω	75 Ω	85 Ω	95 Ω	45 Ω	55 Ω	65 Ω	75 Ω	85 Ω	95 Ω
1	21	30	30	31	31	32	24	27	29	27	27	29
2	13	5	5	3	3	3	9	7	5	7	8	6
3	0	0	0	1	1	0	2	1	1	1	0	0
X	1	0	0	0	0	0	0	0	0	0	0	0

It can be observed that the previous algorithm recorded one undefined case when the fault impedance of 45 Ω was applied at one of the line section, whereas there is no undefined case recorded in the current analysis. This analysis demonstrated the strengths of the current algorithm as compared to the previous one. In addition, the simulation speed of the present algorithm is faster with less storage space and fewer samples (128 samples instead of 256 samples) required, compared to the previous algorithm.

4.1.2. Variation in wavelet families

The different types of mother wavelets have unique properties, but with the same purpose, i.e. to filter out both high and low frequency components from the original signal. These mother wavelets play an important

role where unique features can be extracted using different mother wavelets. These features will then be used as input to the proposed method for locating the faulty section.

The Db4 mother wavelet was proposed in [18] to extract important features from the voltage signal. In this analysis, the mother wavelet will be varied and the accuracy of the algorithm will be analyzed. A total of 3 different wavelet families comprising of Daubechies, Symlet, and biorthogonal at 3 different orders are considered in this study. These mother wavelets are selected based on their reported accuracies from the research conducted in [21]. The same fault simulation is conducted where 6 different HIF values are applied in the middle of each line section for the network as shown in Figure 2. Since each mother wavelet will extract different features, a unique database for each of the mother wavelets needs to be established prior to the fault simulation for computing the AAD scores.

After completing the database development, a case study for faults in the middle of each of the 35 line sections was conducted for different fault impedances. The captured voltage waveform in each of the simulations was analyzed to compute the AAD scores and the faulted line sections were ranked accordingly. After completing all the test fault simulations, the number of correctly ranked line sections for each of the fault impedance values was computed and tabulated, as given in Table 3.

Table 3. Results for different types of mother wavelets.

Rank	Db4						Db6						Db8					
	45 Ω	55 Ω	65 Ω	75 Ω	85 Ω	95 Ω	45 Ω	55 Ω	65 Ω	75 Ω	85 Ω	95 Ω	45 Ω	55 Ω	65 Ω	75 Ω	85 Ω	95 Ω
1	24	27	29	27	27	29	8	22	23	25	30	28	24	28	31	33	34	35
2	9	7	5	7	8	6	5	6	8	6	4	7	2	1	1	2	1	0
3	2	1	1	1	0	0	4	1	0	1	0	0	2	0	2	0	0	0
X	0	0	0	0	0	0	18	6	4	3	1	0	7	6	1	0	0	0

Rank	Sym4						Sym6						Sym8					
	45 Ω	55 Ω	65 Ω	75 Ω	85 Ω	95 Ω	45 Ω	55 Ω	65 Ω	75 Ω	85 Ω	95 Ω	45 Ω	55 Ω	65 Ω	75 Ω	85 Ω	95 Ω
1	21	23	23	26	26	27	19	20	24	22	24	27	31	33	33	33	34	34
2	10	10	9	8	9	8	12	14	10	10	9	8	2	2	2	2	1	1
3	2	2	3	1	0	0	3	1	1	2	2	0	2	0	0	0	0	0
X	2	0	0	0	0	0	1	0	0	1	0	0	0	0	0	0	0	0

Rank	Bior3.3						Bior4.4						Bior5.5					
	45 Ω	55 Ω	65 Ω	75 Ω	85 Ω	95 Ω	45 Ω	55 Ω	65 Ω	75 Ω	85 Ω	95 Ω	45 Ω	55 Ω	65 Ω	75 Ω	85 Ω	95 Ω
1	32	33	32	33	33	33	21	28	31	33	34	34	27	27	27	30	31	32
2	3	2	3	2	2	2	5	7	4	2	1	1	7	7	8	5	4	3
3	0	0	0	0	0	0	2	0	0	0	0	0	1	1	0	0	0	0
X	0	0	0	0	0	0	7	0	0	0	0	0	0	0	0	0	0	0

It can be observed that the accuracy of this algorithm can be assessed either in terms of the lowest number of undefined cases or a higher number of correctly identified faulty sections in rank 1. It is important to note that the fault location and rectification works will be delayed and compromised if any one of the faults is undefined. As such, it is of utmost importance to keep the number of undefined cases as minimal as possible in this faulted section identification algorithm. Due to the above reasons, the selection criteria for the algorithm require that the mother wavelet with the lowest number of undefined cases takes the main priority over a higher number of correctly identified faulty sections in rank 1. This selection criterion was applied to all the studies in this paper.

Table 4 summarizes the results in Table 3. There are 210 cases consisting of 6 different impedances for the HIF and 35 line sections. As shown in the table, only 4 wavelet types (Db4, Sym8, Bior3.3, and Bior5.5) managed to deliver zero undefined cases. As such, these 4 mother wavelets are shortlisted out of the 9 mother wavelets. Although Db8 and Bior4.4 give higher accuracy compared to Db4 and Bior5.5, they were not shortlisted due to the presence of undefined cases.

Table 4. Overall performance for different types of mother wavelets.

Ranking	Db4		Db6		Db8	
1	163	77.62%	136	64.76%	185	88.10%
2	42	20.00%	36	17.14%	7	3.33%
3	5	2.38%	6	2.86%	4	1.90%
X	0	0.00%	32	15.24%	14	6.67%

Ranking	Sym4		Sym6		Sym8	
1	146	69.52%	136	64.76%	198	94.29%
2	54	25.71%	63	30.00%	10	4.76%
3	8	3.81%	9	4.29%	2	0.95%
X	2	0.95%	2	0.95%	0	0.00%

Ranking	Bior3.3		Bior4.4		Bior5.5	
1	196	93.33%	181	86.19%	174	82.86%
2	14	6.67%	20	9.52%	34	16.19%
3	0	0.00%	2	0.95%	2	0.95%
X	0	0.00%	7	3.33%	0	0.00%

Among these 4 wavelet types, only Sym8 and Bior3.3 generated an accuracy of more than 90%. Therefore, Sym8 and Bior3.3 are the highly recommended mother wavelets for this faulted section identification algorithm. However, the findings are not conclusive because the studies in this section considered only faults in the middle of the line section and discrete fault impedance values. Further analysis has to be carried out to verify the performance of the algorithm under dynamic fault conditions. The variations to be studied include change in fault impedance values and change in fault points along the line section. These variations will be discussed in the next section.

4.2. Sensitivity studies

In this section, detailed sensitivity studies for the 4 shortlisted mother wavelets are performed. The sensitivity studies cover variation in faulted point along the line section as well as variation in fault impedance values. Based on the results from the sensitivity studies, the most accurate mother wavelet for this algorithm was identified.

4.2.1. Variation in fault location along the line section

In this subsection, the performances of the shortlisted Db4, Sym8, Bior3.3, and Bior5.5 are analyzed under practical scenarios. The previous sections only considered faults in the middle of the line section. Here the fault is applied at 10%, 25%, 50%, 75%, and 90% of the total line section length. Two different HIF values (45 Ω and 95 Ω) are considered in this analysis. Besides that, the line sections selected for this study are sections

6, 15, 24, and 28. These line sections were chosen because they are located in the branch section, which will complicate the classification process by presenting multiple possible faulty sections to the proposed algorithm.

The rankings of the faulty section as the faulted points are varied are shown in Table 5. It can be observed that higher numbers of undefined cases are recorded when the faulted points are varied in line section 15. In contrast, all fault occurrences at different locations on line section 24 have been successfully identified either in the first or second rank.

Table 5. Results for different points of fault.

Db4										
Section/length	45 Ω					95 Ω				
	10%	25%	50%	75%	90%	10%	25%	50%	75%	90%
6	1	2	2	2	2	1	1	2	2	2
15	3	2	2	X	X	X	3	1	X	X
24	1	1	1	1	2	1	1	1	1	1
28	2	1	2	X	X	X	2	2	3	X

Sym8										
Section/length	45 Ω					95 Ω				
	10%	25%	50%	75%	90%	10%	25%	50%	75%	90%
6	1	1	2	2	2	1	1	2	2	2
15	X	2	1	2	X	X	3	1	X	X
24	1	1	1	1	1	1	1	1	1	2
28	X	1	1	2	1	3	1	1	3	X

Bior3.3										
Section/length	45 Ω					95 Ω				
	10%	25%	50%	75%	90%	10%	25%	50%	75%	90%
6	1	1	2	2	2	1	1	2	2	X
15	X	3	2	X	X	X	X	1	X	X
24	1	1	1	1	1	1	1	1	2	2
28	X	1	1	2	1	X	3	1	2	1

Bior5.5										
Section/length	45 Ω					95 Ω				
	10%	25%	50%	75%	90%	10%	25%	50%	75%	90%
6	1	2	2	2	2	1	1	2	2	2
15	3	2	1	3	X	X	3	1	X	X
24	1	1	1	1	1	1	1	1	1	1
28	1	1	2	2	3	2	1	2	2	2

The results in Table 5 are summarized and shown in Figure 3. The percentages of correctly ranked faulty sections for each of the 4 mother wavelets are shown. The percentage is based on a total of 40 fault simulations (2 different fault impedances × 4 line sections × 5 different fault points). It can be observed that Sym8 achieved the highest accuracy with 50% of the faults being identified in rank 1. In contrast, Bior5.5 achieved the lowest percentage of undefined cases at 10%, followed by Sym8, Db4, and Bior3.3.

Based on the selection criteria presented previously, it can be seen that Bior5.5 achieved the highest accuracies because it recorded the lowest number of undefined cases. It is then followed by Sym8 with 17.5% undefined cases, though it gives higher accuracy compared to Bior5.5. In the previous section, it was observed

that Sym8 and Bior3.3 provided good performance. However, in this analysis Bior5.5 and Sym8 are selected instead of Bior3.3. This is because Bior3.3 recorded the most undefined cases in this sensitivity study.

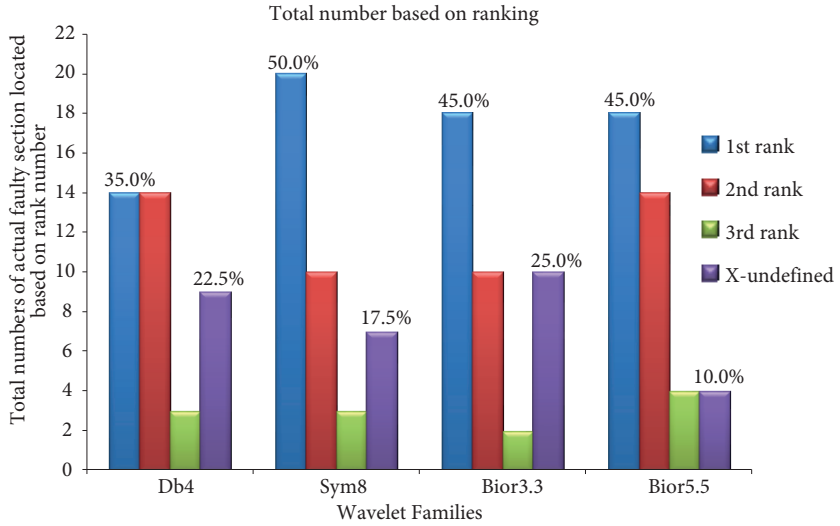

Figure 3. Total numbers of actual faulty section successfully located based on ranking number (variation of fault location).

4.2.2. Variation of fault impedance values

In this section, the accuracies of the algorithm incorporating the 4 mother wavelets under varied fault impedance values are studied. For this purpose, different fault impedance values ranging from 40 to 50 Ω and 90 to 100 Ω, in increments of 1 Ω, are analyzed. All faults in the simulations are applied in the middle of line sections 6, 15, 24, and 28. These line sections are selected to ensure consistency with the previous analysis.

The total percentages of faulty sections successfully located in each rank are depicted in Figure 4. There are 88 simulations consisting of 22 different fault impedance values applied in the middle of 4 different line sections. As shown in the figure, Sym8 delivered the fewest undefined cases, besides delivering the highest accuracy compared to the other mother wavelets. It is followed by Bior3.3, Bior5.5, and Db4.

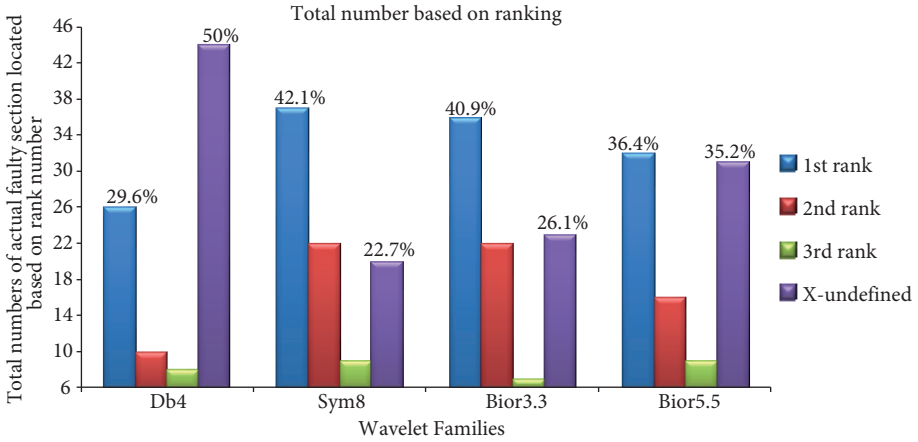

Figure 4. Total numbers of actual faulty section successfully located based on ranking number (variation of fault impedance value).

Even though Sym8 recorded 22.7% of undefined cases, it is still acceptable because around 77% cases can be identified either in the first, second, or third rank. Also, it is challenging to locate all faulty sections when the fault values are varied. However, this issue can be overcome if the number of entries in the database is increased. It must be noted that in this proposed method, the database is established based on fault impedance values of 40 Ω, 50 Ω, 60 Ω, 70 Ω, 80 Ω, 90 Ω, and 100 Ω.

In general, it can be observed that Sym8 has been consistently shortlisted in all the sensitivity studies conducted. The previously proposed Db4 could not deliver the accuracy achieved by Sym8. As such, Sym8 is the recommended mother wavelet to be incorporated into this database faulted section identification algorithm.

In this database fault location technique, 3 different but complementary sources of information can be used to assist the fault location identification [22]. They are system knowledge, data history, and external information. The system knowledge will offer the first 3 faulty section rankings as discussed in the above sections. In the case of an undefined faulty section after checking the third rank, the faulty section can be traced based on the external information and data history. External information such as consumer call, the existence of the construction site, weather conditions, and so on can be useful information to locate the fault. In the unavailability of external information, the data history will then be used to infer possible fault location. In data history, information such as frequency of fault occurrence and previously registered similar behaviors of waveform attributes can be valuable to estimate the faulty section.

5. Conclusion

In this paper, thorough analysis has been carried out to investigate the effect of using a different sampling frequency and window size in predicting the location of a HIF in a distribution network. A single measurement point is utilized to measure the 3-phase voltage signal. The AAD approach is used to rank all possible faulty sections based on the AAD score. With this approach, the extracted features are compared to the values in the databases to predict the faulty section. Furthermore, the effects of using various mother wavelets to predict the faulty section are also studied. A sensitivity study on different fault points along the line section and fault impedance values is also performed. Based on the results, it is shown that the Sym8 mother wavelet delivered better faulty section localization results compared to the other mother wavelets.

Acknowledgments

This work was supported by the University of Malaya, Kuala Lumpur (FRGS Grant No: FP044-2013B) and an e-Science Fund Grant (Grant code: 06-01-03-SF0976)

References

[1] Ali MS, Abu Bakar AH, Mokhlis H, Arof H, Illias HA. Wavelet-based and database approach for locating faulty section of high impedance fault in a distribution system. Prz Elektrotechniczn 2013; 1: 211-218.

[2] Ali MS, Abu Bakar AH, Mokhlis H, Arof H, Illias HA. High-impedance fault location using matching technique and wavelet transform for underground cable distribution network. IEEJ T Electr Electr 2014; 9: 176-182.

[3] Mokhlis H, Li HY, Khalid AR. The application of voltage sags pattern to locate a faulted section in distribution network. Int Rev Electr Eng-I 2010; 5: 173-179.

[4] Coser J, Do Vale DT, Rolim JG. Design and training of artificial neural networks for locating low current faults in distribution systems. In: Intelligent Systems Applications to Power Systems Conference; 5–8 November 2007; Niigata, Japan. New York, NY, USA: IEEE. pp. 1-6.

[5] Thukaram D, Khincha HP, Vijaynarasimha HP. Artificial neural network and support vector machine approach for locating faults in radial distribution systems. IEEE T Power Deliver 2005; 20: 710-721.

[6] Moshtagh J, Aggarwal RK. A new approach to ungrounded fault location in a three-phase underground distribution system using combined neural networks & wavelet analysis. In: Canadian Conference on Electrical and Computer Engineering; May 2006; Ottawa, Canada. New York, NY, USA: IEEE. pp. 376-381.

[7] Ngaopitakkul A, Pothisarn C. Discrete wavelet transform and back-propagation neural networks algorithm for fault location on single-circuit transmission line. In: IEEE International Conference on Robotics and Biomimetics; 22–25 February 2009; Bangkok, Thailand. New York, NY, USA: IEEE. pp. 1613-1618.

[8] Elhaffar AM. Power transmission line fault location based on current traveling waves. PhD, Helsinki University of Technology, Espoo, Finland, 2008.

9 Peretto L, Tinarelli R, Bauer A, Pugliese S. A case study: fault location in underground power networks. In: Innovative Smart Grid Technologies Conference; 17–19 January 2011; Anaheim, CA, USA. New York, NY, USA: IEEE. pp. 1-6.

[9] Navaneethan S, Soraghan JJ, Siew WH, McPherson F, Gale PF. Automatic fault location for underground low voltage distribution networks. IEEE T Power Deliver 2001; 16: 346-351.

[10] Sadeh J, Bakhshizadeh E, Kazemzadeh R. A new fault location algorithm for radial distribution systems using modal analysis. Int J Elec Power 2013; 45: 271-278.

[11] Pourahmadi-Nakhli M, Safavi AA. Path characteristic frequency-based fault locating in radial distribution systems using wavelets and neural networks. IEEE T Power Deliver 2011; 26: 772-781.

[12] Borghetti A, Corsi S, Nucci CA, Paolone M, Peretto L, Tinarelli R. On the use of continuous-wavelet transform for fault location in distribution power systems. Int J Elec Power 2006; 28: 608-617.

[13] Borghetti A, Bosetti M, Di Silvestro M, Nucci CA, Paolone M. Continuous-wavelet transform for fault location in distribution power networks: Definition of mother wavelets inferred from fault originated transients. IEEE T Power Syst 2008; 23: 380-388.

[14] Zhang X, Zeng X, Lei L, Choi SS, Wang Y. Fault location using wavelet energy spectrum analysis of traveling waves. In: International Power Engineering Conference; 3-6 December 2007; Singapore. New York, NY, USA: IEEE. pp. 1126-1130.

[15] Ye L, You D, Yin X, Wang K, Wu J. An improved fault-location method for distribution system using wavelets and support vector regression. Int J Elec Power 2014; 55: 467-472.

[16] Rafinia A, Moshtagh J. A new approach to fault location in three-phase underground distribution system using combination of wavelet analysis with ANN and FLS. Int J Elec Power 2014; 55: 261-274.

[17] Abu Bakar AH, Ali MS, Tan CK, Mokhlis H, Arof H, Illias HA. High impedance fault location in 11kV underground distribution systems using wavelet transforms. Int J Elec Power 2014; 55: 723-730.

[18] MathWorks. Wavelet Toolbox User's Guide for Use with MATLAB. Natick, MA, USA: MathWorks Inc., 2009.

[19] Lim PK, Dorr DS. Understanding and resolving voltage sag related problems for sensitive industrial customers. In: IEEE 2000 Power Engineering Society Winter Meeting; 23–27 January 2000; Singapore. New York, NY, USA: IEEE. pp. 2886-2890.

[20] Avdakovic S, Nuhanovic A, Kusljugic M, Music M. Wavelet transform applications in power system dynamics. Electr Pow Syst Res 2012; 83: 237-245.

[21] Mora-Flòrez J, Meléndez J, Carrillo-Caicedo G. Comparison of impedance based fault location methods for power distribution systems. Electr Pow Syst Res 2008; 78: 657-666.